ELSEVIER

Catalysis Today 51 (1999) 255–268

CATALYSIS TODAY

Structure–reactivity relationships in oxidation of C_4 hydrocarbons on supported vanadia catalysts

Vadim V. Guliants*

PRAXAIR, Inc., 175 East Park Drive, Tonawanda, NY 14151, USA

Abstract

Molecular vanadia species supported on the surface of metal oxides are used as catalysts for many hydrocarbon oxidation reactions. This paper discusses (i) the structure of the surface vanadia species in fresh and dehydrated catalysts, (ii) the structural and oxidation state changes during C4 hydrocarbon oxidation, and (iii) the roles of the oxide support, the surface oxygen species, and the acidity of the supported vanadia catalysts in selective oxidation catalysis. The molecular structure and reactivity information provides new fundamental insights into the catalytic properties of surface vanadia species during C4 hydrocarbon oxidation. On the other hand, the studies of the model supported vanadia catalysts shed new light on the origins of the catalytic activity of the bulk vanadium–phosphorus oxide (VPO) catalysts for partial oxidation of *n*-butane to maleic anhydride. The new fundamental structure–activity and selectivity relationships of surface vanadia species on oxide supports provide a foundation for the molecular engineering of supported catalysts for selective oxidation of hydrocarbons. © 1999 Elsevier Science B.V. All rights reserved.

Keywords: Structure–reactivity; C_4 hydrocarbons; Supported vanadia catalysts

1. Introduction

Supported metal oxide catalysts consist of an active metal oxide component, e.g. vanadia, deposited at the surface of an oxide support, such as SiO_2, TiO_2 and Al_2O_3. Currently, considerable interest is devoted to studying selective oxidation of alkanes on supported vanadia catalysts. The selective oxidation of alkanes is highly desirable due to their potentially low environmental impact and the relatively low cost of raw materials. Some typical systems being studied are partial oxidation of *n*-butane to maleic anhydride on supported vanadium–phosphorus oxide catalysts (VPO) [1–16], and oxidative dehydrogenation of *n*-butane [17–19]. Many fundamental questions still remain unanswered about supported vanadia catalysts despite the importance of this catalytic system. Progress in understanding the fundamentals of the supported vanadia catalysts is hindered primarily by

1. the presence of impurities, such as P and K, in the oxide supports,
2. studies comparing the catalysts under ambient and in situ conditions, and
3. the limitations of the bulk characterization techniques in studying surface phenomena.

The goal of this paper is to address several fundamental issues about C_4 hydrocarbon oxidation on supported vanadia catalysts:

*Tel.: +1-716-879-7006; fax: +1-716-879-7030; e-mail: vadim_guliants@praxair.com

0920-5861/99/$ – see front matter © 1999 Elsevier Science B.V. All rights reserved.
PII: S0920-5861(99)00049-8

1. molecular structures of vanadia species in fresh catalysts,
2. molecular structures of vanadia species in catalysts under reaction conditions,
3. the role of oxide support and metal oxide additives on structure and reactivity.

These issues are of primary importance for establishing structure–property relationships in C_4 hydrocarbon oxidation on supported vanadia catalysts and also have important implications for the bulk, i.e. unsupported, catalytic VPO system.

2. Molecular structure of vanadia species in fresh catalysts

Molecular structure of supported vanadia catalysts is a strong function of the surface coverage. Surface coverage of vanadia overlayer supported on metal oxides has been determined experimentally [20,21] and via structural calculations [22,23]. Experimental determinations of the surface coverage are done using several spectroscopic techniques, such as Raman, IR, XPS, ^{51}V NMR and UV–Vis DRS, as well as temperature-programmed reduction (TPR) and redox reactions. Among these techniques, Raman spectroscopy is particularly discriminating between the surface vanadia species and the crystalline V_2O_5. Characteristic Raman bands of polymeric vanadia species corresponding to the V–O–V stretches, appear below 1000 cm^{-1} at high coverages, while the isolated vanadate species present at submonolayer coverages produce only one Raman band of the terminal V=O bond at 1020–1040 cm^{-1}. The fingerprint Raman features allow detecting monolayer formation immediately prior to appearance of crystalline V_2O_5. Based on Raman spectroscopy measurements, monolayer surface coverage on a number of oxide supports (Al_2O_3, TiO_2, ZrO_2, Nb_2O_5 and CeO_2) was found to be 7–8 VO_x per nm^2 [21,24]. Vanadia supported on silica exhibited unusually low monolayer surface coverage of only ca. 0.7 VO_x per nm^2. Lower density and reactivity of the hydroxyls explain such low monolayer surface coverage on the silica surface, which anchor vanadia species to the support.

The structural calculations of monolayer surface coverage assume similarity between the structures of crystalline bulk and surface vanadia. Based on crystal structure of V_2O_5, the monolayer surface coverage corresponds to 4.98 molecules of V_2O_5 per nm^2 [25]. From the V–O bond length of crystalline V_2O_5, monolayer surface coverage is estimated at 10 VO_x per nm^2 for a 2D polyvanadate layer and at 2.5 VO_x per nm^2 for isolated monomeric vanadia species [22,23]. Comparison between experimental (7–8 VO_x per nm^2) and theoretical monolayer coverages suggest that the surface vanadia species are present as a closely packed monolayer at the surface of oxide supports. The above-mentioned estimates are based on well-characterized supports containing no surface impurities. However, commercial grade supports, such as pigment grade titania, typically contain monolayer quantities of P, Na, K, Ca, etc., which interact with surface vanadia to form an amorphous phase [26]. In such systems, the surface vanadia titrates both the oxide support and the surface impurities, delaying formation of crystalline V_2O_5 until several vanadia monolayers are formed. Thus, the observed ''monolayer'' vanadia coverage in such impurity-containing systems can be 2–4 times greater than that found above for the well-defined supported catalysts.

A number of synthesis methods were used to prepare supported vanadia catalysts, such as incipient impregnation with vanadium oxalate [27], ammonium metavanadate and phosphate [14], aqueous solution of $VO(H_2PO_4)_2$ [15], aqueous solution of V(III) and phosphoric acid [9,10], vapor phase grafting with $VOCl_3$ [28,29], ammonium metavanadate [29], non-aqueous impregnation with vanadium alkoxides [24,26] or V(V) and P(V) sources [7], and dry mixing with crystalline V_2O_5 [30]. Aqueous impregnation with vanadium oxalate is favored in commercial preparations due to its high solubility in water and the absence of undesirable volatile organic solvents. Under ambient conditions the supported catalysts contain multilayers of adsorbed water. Under such conditions the bridging V–O-support bonds are hydrolyzed and the hydrated vanadia species are dissolved in the thin aqueous layer. The corresponding structural changes can be detected by Raman spectroscopy [21], ^{51}V NMR [31,32], ESR [33], and UV–Vis DRS [34]. Depending on the concentration of vanadia species and the pH of the aqueous film determined by the point of zero charge of the oxide support, metavanadate $(VO_3)_n$, orthovanadate (VO_4^{3-}), pyrovanadate

($V_2O_7^{4-}$), and decavanadate ($V_{10}O_{28}^{6-}$) can be detected.

Supported VPO catalysts represent a special case where depending on the nature of the oxide support, either well-dispersed molecular or (micro)-crystalline VPO species are observed [6,14–17]. Acoustophoresis has been recently applied to study reactions of vanadium and phosphate ions in aqueous solution with the surface of titania, alumina and silica supports [35]. This technique allows to study formation of suspended colloidal particles from ions in solution by monitoring the changes in the acoustic response of the system to an electric field [36]. In this method, an amplitude of the acoustic wave generated in solution by an electric field called the electrokinetic sonic amplitude (ESA) is measured. The ESA is produced by both the ions and colloidal particles present in solution. Therefore, the two components of ESA are termed the ionic and the colloid vibration potential, IVP and CVP, respectively. The acoustophoretic measurements of the ESA allow to determine the isoelectric point (IEP) of the system as a function of the oxide support. Comparison of the IEPs measured in the presence and absence of the vanadium ions in solutions provide information about the state of the surface and the nature of vanadium species interacting with the surface. In this study [35], the extent of interaction of the dissolved VPO precursor with the silica support was found to be small, which resulted in formation of unsupported bulk VPO material. The high affinity of alumina towards phosphate resulted in a supported, phosphate depleted VPO phase. The phosphate depletion effect was less pronounced in the case of titania, and a well-dispersed VPO phase was obtained [35].

The influence of the various preparation methods on the structure of supported catalysts was studied by Wachs et al. [37]. They studied a series of vanadia catalysts supported on titania under ambient and dehydrated conditions by Raman spectroscopy and ^{51}V NMR. The authors [37] found that after prolonged calcination the structure of the vanadia species in all the catalysts was identical regardless of the synthesis method. High mobility of surface vanadia species and the strong driving force to minimize the free energy of the supported oxide system by spreading vanadia species explain the lack of influence of preparation methods.

3. Molecular structure in dehydrated state

The moisture adsorbed in supported vanadia catalysts under ambient conditions may be removed by heating supported catalysts in nonreducing oxygen-containing atmosphere at elevated temperature, 573–973 K. Such treatment also helps maintain the 5+ oxidation state of the surface vanadia species. At temperatures below 473 K, the Raman stretch of the terminal V=O bond occurring at 1020–1040 cm^{-1} is shifted significantly downward due to extensive hydration of the surface vanadia. At temperatures above 473 K a small amount of moisture hydrogen-bonded to surface vanadia results in a few cm^{-1} downward shift of the Raman V=O band. At these temperatures ^{18}O labeling experiments showed that the reversibly adsorbed moisture is also capable of rapidly undergoing ^{18}O exchange with the terminal V=O bonds.

The dehydrated surface vanadia species on most commonly studied metal oxide supports (Al_2O_3, TiO_2, ZrO_2, Nb_2O_5 and CeO_2) possesses essentially identical molecular structures found by IR [20,38,39], Raman [20,39–41], ^{51}V NMR [32,42], and EXAFS/XANES [43,44]. These structural studies suggested that the dehydrated vanadia species on these supports was predominantly present as isolated and polymeric tetrahedral VO_4 units (Fig. 1). In the case of vanadia overlayer supported on alumina, polymeric tetrahedral VO_4 species were predominant at low surface coverages (5 wt% or under 40% of the monolayer coverage) [19]. The concentration of distorted octahedral V(V) species was found by ^{51}V NMR to increase at surface vanadia coverage above half the monolayer [19]. ^{18}O labeling experiments showed that these surface species possessed only one terminal V=O bond [45,46]. The current structural model assigns one terminal V=O bond and 3 bridging V–O-support

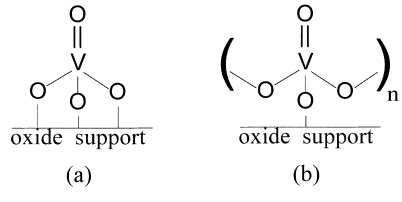

Fig. 1. Molecular structure of dehydrated isolated (a) and polymerized (b) vanadia species on oxide supports.

bonds for the isolated species, while the polymeric surface species has only one V–O-support bond per vanadium atom, the other two being bridging V–O–V bonds (Fig. 1).

By contrast, vanadia species supported on silica consist exclusively of isolated tetrahedral VO_x groups possessing three bonds to support and one terminal V=O bond. The longer V–O(support) and shorter V=O bond lengths in such tetrahedral species were determined to be 1.79 and 1.60 Å, respectively, in a recent EXAFS study (Table 1 [47]). Incidentally, the maximum reported surface vanadia coverage on silica corresponds to that shown above for isolated VO_x species [22,23,31]. Microcrystalline V_2O_5 is detected on vanadia-supported silica by Raman spectroscopy at higher surface coverages at 994, 702 and 527 cm^{-1}.

Unlike the aforementioned supported catalysts, the magnesia-supported vanadia catalysts are characterized by partial dissolution of vanadate species in the MgO bulk. This results in formation of a bulk V–Mg–O mixed metal oxide in addition to surface vanadia species [42]. The vanadium coordination in these mixed metal oxide phases ranges from tetrahedral and square pyramidal to octahedral.

4. Structural changes during hydrocarbon oxidation

Several studies addressed the structural and oxidation state changes in supported vanadia catalysts during hydrocarbon oxidation reactions [11,48,49]. During typical methane oxidation reaction, the vanadia species remain predominantly in the 5+ oxidation state and possess the same structure reported for dehydrated conditions [48]. In the absence of oxygen, methane only slightly reduces vanadium present on TiO_2 and CeO_2 supports, while no reduction is detected in the case of V_2O_5/SiO_2 system. This experimental observation reflects high C–H bond energy in methane molecule. During butane oxidation to maleic anhydride the Raman signal of the surface V(V) species decreased 10–35% reflecting partial reduction of the vanadia species under reaction conditions, with the exception of the V_2O_5/SiO_2 system [11,16]. In the absence of oxygen, the surface vanadia species on alumina were completely reduced by butane under reaction conditions. The average oxidation state of vanadium in VO_x/TiO_2 catalyst for partial oxidation of *n*-butane was found to be near +4.5. By comparison the average oxidation state of vanadium in VO_x/Al_2O_3 after oxidative dehydrogenation (ODH) of *n*-butane to C_4-olefins was much lower, +3.1 to +3.8 (Table 1 [19]). Lower oxidation state of vanadium in these catalysts may be related to greater reducing power of the oxygen-lean feed during ODH and considerably higher reaction temperature [19]. The reducibility of the surface vanadia species during butane oxidation on various oxide supports follows the order: TiO_2>CeO_2>ZrO_2>Al_2O_3>SiO_2. However, the surface vanadia coverage was also found to be a critical variable since the polymeric surface vanadia species present at high surface coverage are more easily reduced than the isolated surface vanadia species. The surface vanadia species are even more extensively reduced during butene oxidation than butane oxidation manifested in reduction of the V(V) on silica support [11,16]. Thus in situ Raman spectroscopy provided new insights into the behavior of surface vanadia species during hydrocarbon oxidation reactions:

1. the dehydrated surface V(V) species appears to be the predominant surface species,
2. the extent of reduction of the surface vanadia species depends on the reducing power of the hydrocarbon, the specific oxide support and the ratio of polymeric to isolated surface vanadia species [50].

In situ Raman spectroscopy did not provide any insights into the molecular structure of the reduced surface V(IV) and V(III) species formed during the hydrocarbon oxidation, since no new Raman bands were observed [11,48]. It appears that the reduced V(IV) and V(III) species in the supported vanadia catalysts do not produce strong and detectable Raman signals. Such structural information about the reduced surface vanadia species present under reaction conditions can be gathered from UV–Vis DRS for V(IV) and V(III) [34,51,52] and in situ ESR for isolated V(IV) [19,22,34,52]. The published UV–Vis DRS studies only report oxidation states and do not discuss the coordination of the reduced surface vanadia [51,52]. The published ESR studies have reported various geometries for V(IV) species in supported

vanadia catalysts: distorted octahedral VO_6, square-pyramidal VO_5 or trigonal–pyramidal VO_4 V(IV) species. However, due to the complexity of supported vanadia system these structural assignments are not very certain. Therefore, more detailed ESR studies of well-defined model supported vanadia catalysts are required to reliably extract the fundamental coordination information about the reduced surface V(IV) species.

In the case of VPO catalysts supported on silica (Fig. 4 [14]) only slight changes in the average oxidation state of vanadium were detected by the XANES technique after *n*-butane oxidation. The P/V=1 supported catalysts remained as V(V) phase, while phosphorus enrichment in the P/V=1.95 catalyst containing V(IV) stabilized lower 4+ oxidation state of vanadium. These observations are consistent with the bulk nature of the active VPO component in these catalysts [53]. The weak interaction between the non-reducible silica support and the surface VPO component was found to affect the reducibility of the VPO matrix in another study [10]. Reducibility of the VPO component in these catalysts inversely correlated with the surface coverage, which may be related to the degree of dispersion and average size of the VPO particles supported on silica (Figs. 4 and 5 [10]). To the contrary, when the VPO was supported on a reducible support such as titania, the reducibility under reaction conditions increased with surface coverage (Figs. 6–8 [9]). The surface VPO phase strongly interacted with the titania support and its dispersion increased during exposure to the reaction feed.

Ruitenbeek et al. [8] studied the changes in the vanadium oxidation state during the equilibration of the titania-supported VPO catalysts by the XANES technique. They observed that after a few redox cycles, the titania-supported VPO catalyst was equilibrated, i.e. no changes in the average vanadium oxidation state were taking place. At first, the freshly oxidized catalyst displayed changes in both the vanadium K-edge and the pre-edge corresponding to an increase in the vanadium oxidation state (Fig. 4 [8]). Vanadium was reduced after the catalyst was exposed for the first time to *n*-butane at 553 K in the absence of oxygen (Fig. 5 [8]). The subsequent redox cycles led to no observable changes in the vanadium oxidation state (Fig. 6 [8]).

5. Structure–activity relationships in oxidation of C_4 hydrocarbons

Several studies of C_4 hydrocarbon oxidation have been reported in the literature [1–7,11,17,54,55]. Owens and Kung [17] studied *n*-butane dehydrogenation on silica-supported vanadia catalysts at 793 K. They observed that the isolated vanadia species present at low surface coverage (0.53 and 0.58 wt% V) were responsible for the high total dehydrogenation selectivity (1-butene, *cis-/trans*-2-butene, and 1,3-butadiene in Fig. 6 of [17]). The presence of the crystalline V_2O_5 species at high surface coverage (998, 703, 526, 480, 404, 304 and 284 cm^{-1} Raman bands for the 6.4 wt% V catalyst in Figs. 4 and 5 of [17]) contributed to the production of total oxidation products. Mori et al. [50] studied oxidation of *n*-butane on titania-supported vanadia catalysts at high temperature (693–763 K) and high butane conversion. Such severe experimental conditions led to an overoxidation of *n*-butane to carbon oxides and, likely, to combustion of the partial oxidation products, including maleic anhydride (Table 2 in [54]). They found that the reaction rate under such conditions was proportional to the amount of V^{5+}=O species in the catalyst (Fig. 5 in [54]), and concluded that the reaction proceeded via the reduction–oxidation or Mars–van Krevelen mechanism according to which the surface V=O species contained the active oxygen. Busca et al. [55] employed titania-supported vanadia catalysts in *n*-butane oxidation and observed overoxidation of the hydrocarbon on very active high surface area catalyst (117 m^2/g) at 723 K. When they supported 10 wt% V_2O_5 on the low surface area titania (18.4 m^2/g), vanadia formed microcrystals which were detrimental to selective oxidation and led to *n*-butane combustion. A number of studies of supported VPO catalysts have been described in the literature [1–7]. Nakamura et al. [1] studied oxidation of 1-butene on alumina-supported catalysts and reported reasonably high selectivities to maleic anhydride. The results of their study [1] showed that supported VPO catalysts could selectively oxidize C_4 hydrocarbons to maleic anhydride. They concluded that the activity and selectivity of their supported catalysts for the oxidation of 1-butene to maleic anhydride were closely related to the oxidation state and the degree of aggregation of vanadium ions. Nakamura et al. [1]

implicated the V^{4+}–V^{5+} redox mechanism of oxidation in which V=O bonds played an important role. Trifiró et al. [56] studied oxidation of butadiene on VPO catalysts supported on zeolites HY (Si/Al=2.1) and HZSM-11 (Si/Al=49). In the case of a hydrophobic high silica zeolite HZSM-11, they found that the VPO component aggregated on the outside surface of the HZSM-11 crystallites. On the other hand, the VPO component was well dispersed inside the supercages of the more hydrophilic zeolite HY and interacted with the Brønsted OH groups. Different nature of the VPO species in these catalysts resulted in the formation of different oxidation products: the expected maleic anhydride in the case of the VPO/HZSM-11 system, and furan in the case of the VPO/HY catalyst [56]. Martinez-Lara et al. [6] synthesized vanadyl phosphate in the presence of titania and silica. In the case of silica support, α-$VOPO_4$ formed without any indication of silica-VPO interaction. This system exhibited very low catalytic activity similar to unsupported bulk α-$VOPO_4$ [57]. On the contrary, an amorphous VPO (P/V=1) layer covered the surface of the titania support, preventing crystallization of $VOPO_4$ up to 21% of the VPO content. Despite the high activity of the titania-supported system in *n*-butane oxidation, only total combustion products were observed [6].

Kung et al. [14] observed the bulk α_I-$VOPO_4$ phase supported on silica at monolayer coverage by both XRD and Raman spectroscopy (Figs. 1 and 2 in [14]). At the P/V ratio of 1.95 in the supported catalysts the bulk $VO(PO_3)_2$ phase was also detected in addition to α_I-$VOPO_4$ [14]. $VO(H_2PO_4)_2$ in the silica-supported catalysts transformed into a highly disordered $VO(PO_3)_2$ phase under catalytic conditions [14,15,57]. Earlier studies identified this phase as inactive in butane oxidation [57]. Recently, Kung et al. [58] studied oxidation of *n*-butane on vanadia catalysts supported on hydrophobic and hydrophilic silica surfaces at various synthesis P/V ratios. Kung et al. [58] observed that the crystalline VPO phases were formed on both types of support at the above monolayer surface coverages. In the catalysts prepared at the synthesis P/V>2 in the aqueous medium, $VO(PO_3)_2$ phase was detected again. High temperature employed during the P/V=1.1 catalyst activation and kinetic studies (748 and 823 K) resulted in complete overoxidation of the V(IV) precursors into V(V) phosphates. Subsequent reduction of these oxidized catalysts in nitrogen at 1043 K resulted in the appearance of crystalline vanadyl(IV) pyrophosphate. The hydrophilic silica support stabilized the oxidized $VOPO_4$ phases in a P/V=1.1 catalyst (Figs. 4–8 in [58]), and no reduction to vanadyl(IV) pyrophosphate was observed. However, even the P/V=1.1 catalysts which contained $(VO)_2P_2O_7$ remained relatively unselective to maleic anhydride: the selectivity to maleic anhydride was 19–27% at 10–33% *n*-butane conversion at 698 K (Table 3 [58]). Kung et al. [58] explained such poor catalytic behavior by a specific surface termination of the $VOPO_4$-derived $(VO)_2P_2O_7$ phase with V^{5+} species which were less selective in *n*-butane oxidation. On the other hand, the catalytic activity of the aqueous supported catalysts was inversely proportional to the synthesis P/V ratio, indicating that the $VO(PO_3)_2$ phase which dominated at high P/V ratios was inactive in *n*-butane oxidation (Table 2 [58]).

Zazhigalov et al. [2] immobilized the VPO component by adsorption of V(V) and P(V) sources onto the silanol groups of silica support in nonaqueous medium. The formation of the amorphous VPO clusters improved selectivity to maleic anhydride. The *n*-butane conversion and selectivity to maleic anhydride depended on the P/V ratio employed during synthesis, which the authors related to the changes in acidity [2]. Other studies conducted on silica-, alumina-, and $AlPO_4$-supported catalysts [3–5,7] demonstrated further that the acidity of supported catalysts depends on the nature of the support used and that the selectivity to maleic anhydride is affected by the average valence state of vanadium.

Overbeek et al. [9,10] recently studied the role of the silica and titania supports in *n*-butane oxidation to maleic anhydride on supported VPO catalysts. In the case of the titania-supported catalysts, the precipitated VPO phase was amorphous and well-dispersed over the surface of the support as seen in the absence of fine structure in the DRIFT spectra and HRTEM images (Figs. 2, 4 and 5 [9]). The XPS measurements (Table 2 [9]) showed that the surface of the P/V=1.1 titania-supported catalysts was enriched in phosphorus (P/V=1.2–3.0) similar to the bulk VPO catalysts (typically, P/V=1.1–1.7). The authors [9] calculated the thickness of the VPO component in the titania-supported catalysts to be between 0.7 and 2.3 nm. The supported nanophase VPO catalysts showed activity

and selectivity in *n*-butane oxidation at temperatures ca. 100 K lower than commercial VPO catalysts. For example, a 2.9 wt% V loaded catalysts possessing a P/V ratio of 2.0 possessed the selectivity to maleic anhydride of 50 mol% at 10% butane conversion. The inverse relationship between the surface P/V ratio and the catalytic activity found in this supported catalytic system was similar to that in the bulk VPO. Overbeek et al. concluded that the activity of titania-supported VPO catalysts was related to several characteristics:

1. the high surface area,
2. the strong interaction of the VPO component with the titania support,
3. their reducibility based on the results of the temperature-programmed reduction (TPR) experiments (Figs. 6 and 7 [9]), as well as to
4. the average oxidation state of vanadium ions on the surface [9,10].

The VPO component in the silica-supported catalysts was also well-dispersed, but interacted weakly with the support surface as compared to the titania-supported system (TPR curves in Fig. 4 [10] and Fig. 6 [9]). In contrast to the titania-supported VPO system, the silica-supported VPO catalysts were less active, but more selective to maleic anhydride [10]. Overbeek explained lower catalytic activity of the silica-supported system by the non-reducible nature of silica support [10]. However, higher surface P/V ratios found in the silica-supported catalysts as compared to the titania-supported system (Table 2 [10] versus Table 2 [9]) may also be responsible for lower activity in *n*-butane oxidation and higher selectivity to maleic anhydride at high conversion in these catalysts (Figs. 6 and 7 [10] versus Figs. 9 and 10 [9]). Ruitenbeek et al. [8] further studied the changes in the vanadium oxidation state during the equilibration of the titania-supported VPO catalysts in the pulse-flow experiments by in situ XANES spectroscopy. They observed that after a few redox cycles, the titania-supported VPO catalyst was equilibrated, i.e. no changes in the average vanadium oxidation state were taking place (Figs. 4–6 [8]). Since the vanadium oxidation state did not change during *n*-butane oxidation, Ruitenbeek et al. [8] concluded that the lattice VPO oxygen species was not involved in *n*-butane oxidation. According to Ruitenbeek et al. [8], the Mars–van Krevelen mechanism of *n*-butane oxidation was not operative for the titania-supported VPO catalysts due to the lack of change in the vanadium oxidation state during the two-step oxidation–reduction process.

Further studies addressed fundamental structure–reactivity relationships for the C_4 hydrocarbon oxidation on well-defined supported catalysts by specifically probing the nature of active surface oxygen species, the role of the oxide support and various acidic additives. The findings of these studies are discussed in detail below.

6. Role of surface oxygen species

The terminal V=O oxygen has been proposed by many investigators to be the active oxygen involved in hydrocarbon oxidation over supported vanadia catalysts. However, the combination of in situ Raman and hydrocarbon oxidation reactivity studies have recently suggested that the reaction properties are not related to the characteristics of the terminal V=O bonds in supported vanadia catalysts. Butane oxidation over a series of supported vanadia catalysts was found to vary by over an order of magnitude in TOF (Table 1 [16]), but identical V=O Raman features were observed for these catalysts (V=O stretch at 1025–1032 cm^{-1} in Figs. 1–9 [16]). Furthermore, ^{18}O-labeling of the terminal V=O bond during butane oxidation revealed that this bond is very stable and has an exchange time that is approximately 20 times longer than the characteristic reaction time [11]. The ^{18}O-labeled 4 wt% V_2O_5/ZrO_2 catalyst exhibited the V=^{18}O Raman stretch at 983 cm^{-1} which disappeared only after 25 min of *n*-butane oxidation (Fig. 10 [16]). Therefore, the available data suggests that the terminal V=O oxygen is not involved in kinetically significant reaction steps of hydrocarbon oxidation over supported vanadia catalysts.

The surface concentration of bridging V–O–V bonds increases with surface vanadia coverage due to the increase in the ratio of polymerized to isolated surface vanadia species (Fig. 1). The V_2O_5/SiO_2 system represents one notable exception to this rule, since microcrystalline V_2O_5 is formed at above monolayer coverage (Fig. 1 [16]). The TOF for the oxidation of butane to maleic anhydride over V_2O_5/TiO_2 system was found to slightly increase, by a factor of 2–3, with surface vanadia coverage (Fig. 2) because of the

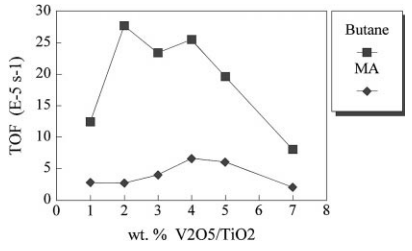

Fig. 2. Oxidation of *n*-butane on supported vanadia catalysts as a function of vanadia surface coverage. Conditions: oxidation of 1.2 vol% *n*-butane in air on the V_2O_5/TiO_2 system at 494 K.

requirement of several surface vanadia sites for this hydrocarbon oxidation reaction [11]. It appears that the bridging V–O–V bonds do not significantly influence this and many other oxidation reactions [59]. However, more systematic studies employing well-defined model supported vanadia catalysts are required to fully understand the role of bridging V–O–V bonds in hydrocarbon oxidation reactions.

During butane oxidation to maleic anhydride the Raman signal of the surface V(V) species decreased 10–35% reflecting partial reduction of the vanadia species under reaction conditions (V=O and V–O–V stretches in Figs. 1–9 [16]). The average oxidation state of vanadium in the selective VO_x/TiO_2 catalyst for partial oxidation of *n*-butane was found to be near +4.5. The surface vanadia coverage was also found to be a critical variable as the polymeric surface vanadia species present at high coverage are more easily reducible than the isolated vanadia species. The reducibility of the surface vanadia species during butane oxidation on various oxide supports followed the order: TiO_2>CeO_2>ZrO_2>Al_2O_3>SiO_2 (Figs. 1–9 [16]). However, the butane oxidation TOF was not found to correlate with the extent of reduction of the surface vanadia species (Figs. 1–9 and Table 1) [16]. The maleic anhydride selectivity did not appear to directly correlate with the extent of reduction either, since the selectivity pattern was Al_2O_3>Nb_2O_5>TiO_2>SiO_2>ZrO_2∼CeO_2 (Table 1 [16]).

Varying the specific oxide support or oxide support ligands without changing the structure of the surface vanadia species can alter the characteristics of the bridging V–O-support bond. The bridging V–O-support bond appears to be associated with the critical oxygen required for hydrocarbon oxidation reactions since changing the specific oxide support dramatically affects the TOF: approximately two orders of magnitude for *n*-butane oxidation to maleic anhydride (Table 1 [16]). The general trend appears to be CeO_2>ZrO_2∼TiO_2>Nb_2O_5>Al_2O_3>SiO_2, which inversely correlates with the Sanderson electronegativity of the oxide support cations [60]. This suggests that bridging oxygens in the V–O-support bonds that are more electronegative or basic, corresponding to oxide support cations with lower electronegativity, are associated with the critical oxygen required for hydrocarbon oxidation reactions over supported vanadia catalysts. The formation of the V–O–P bond has a particularly positive effect on the butane oxidation TOF and maleic anhydride selectivity (Table 3 [16]). The 1% V_2O_5/5% P_2O_5/TiO_2 catalyst displayed the highest selectivity to maleic anhydride among all systems studied (Table 3 [16]). At 494 K in 1.2 vol% *n*-butane in air and 12.1 mol% *n*-butane conversion, the selectivity to maleic anhydride reached 56.2 mol%. Such catalytic behavior is consistent with the above observation that bridging V–O-support bonds are critical in the oxidation of *n*-butane to maleic anhydride. This is also in agreement with recent electron microscopy results revealing that the V–O–P oxygen may be selectively abstracted during reduction of the bulk VPO catalysts by *n*-butane [61].

The insight into the number of critical surface vanadia sites required in hydrocarbon oxidation reactions can be gained by examination of the variation of the TOF with surface vanadia coverage. Those reactions that require only one surface site will exhibit a TOF that is independent of surface vanadia coverage. The oxidation of butane to maleic anhydride over titania-supported vanadia catalysts (Table 2 and Fig. 11 [16]) exhibited an increase in TOF with surface vanadia coverage [11,16]. This may reflect the requirement of multiple surface vanadia sites or the influence of other factors, such as surface acidity influence of bridging V–O–V bonds, structural changes, etc. Some of these factors can be distinguished with the addition of metal oxide additives to the supported vanadia catalysts as discussed below. Similar observations were made during *n*-butane oxidation on silica-supported VPO catalysts [14].

Information about the number of surface sites required for hydrocarbon oxidation reactions can be also probed by the addition of noninteracting surface metal oxides. Noninteracting metal oxides preferen-

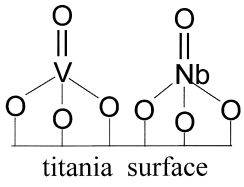

Fig. 3. Molecular structure of supported vanadia catalysts containing noninteracting surface metal oxides, such as Nb_2O_5.

tially coordinate with the oxide support rather than the surface vanadia species under dehydrated conditions (Fig. 3). Typical noninteracting oxides are surface oxides of W, Nb, S, Si, Mo, Ni, Co and Fe [26,62,63]. Noninteracting metal oxides only indirectly affect the molecular structure of the surface vanadia species via lateral interactions. Such lateral interactions influence the relative concentrations of polymerized and isolated vanadia species in supported metal oxides. Interacting acidic oxides, such as P_2O_5 significantly increase the TOF for butane oxidation to maleic anhydride [11,16]. The enhancement in butane oxidation TOF and maleic selectivity upon introduction of acidic oxides further confirms the positive role of acidity in this reaction. The butane oxidation TOF was increased by a factor of 2 and 3 when acidic metal oxides, such as WO_3 and Nb_2O_5, were introduced to the V_2O_5/TiO_2 system (Table 3 [16]). For example, introduction of surface niobia species to V_2O_5/TiO_2 catalysts led to a threefold increase in the TOF for the oxidation of butane to maleic anhydride [11,16]. This increase in TOF also reflects the requirement of multiple surface metal oxide sites for this hydrocarbon oxidation. In contrast to noninteracting additives that mainly affect oxidation reactions requiring multiple surface sites, interacting additives affect all hydrocarbon oxidation reactions since they directly alter the structure and reactivity of the surface vanadia sites. Interacting metal oxides, especially basic oxides, retard the reduction of surface vanadia species. Consequently, the TOF for all hydrocarbon oxidation reactions are lowered when basic additives are introduced [26,64].

7. Role of acidity of supported vanadia catalysts

The oxide supports possess only surface Lewis acid sites, with the exception of silica where no Lewis acid sites exist on the surface. The relative Lewis acid strength of these sites follows the order Al_2O_3>Nb_2O_5>TiO_2>ZrO_2. In contrast to the oxide supports, unsupported V_2O_5 crystalline powders displays both surface Brønsted and Lewis acid sites [65]. The formation of the surface vanadia species on the oxide supports is accompanied by a decrease in the number of surface Lewis acid sites, e.g. measured as the intensity of the $1450\,cm^{-1}$ IR band of adsorbed pyridine (Table 1 [19]), and an increase in the number of surface Brønsted acid sites [19,66,67]. Only a very small fraction of the surface vanadia species are also surface Brønsted acid sites since the concentration of surface Brønsted acid sites measured by pyridine adsorption, corresponds to only 5–10% of the surface vanadia species at monolayer coverage. The Brønsted acid sites present on the surface of the V_2O_5/Al_2O_3 catalysts in a recent study were related mainly to octahedral V(IV) species detected in the ESR spectra (Fig. 7 [19]). The exact location of the surface Brønsted acid sites is not clear at present since solid state ^1H NMR studies cannot clearly discriminate between different environments due to similar NMR peak chemical shifts [68]. Several in situ IR studies have assigned an OH vibration for dehydrated V_2O_5/TiO_2 system to Brønsted V–OH sites [69,70]. However, for well-defined model supported vanadia catalysts, no OH vibrations are observed at monolayer coverage due to titration of the support surface hydroxyls by the surface vanadia overlayer [66]. The acidic characteristics of the surface vanadia overlayer are influenced by the specific oxide support ligand, but the molecular structural characterization studies revealed that excluding silica, the same dehydrated surface vanadia species are present on all the oxide supports. This suggests that the surface Brønsted hydroxyls may be located as bridging-V–OH-support sites, but no direct spectroscopic evidence is currently available to support any assignment for the location of the surface Brønsted acid site [50]. Reduction of the surface vanadia species removes the surface Brønsted acid sites which are only present for the oxidized V(V) surface vanadia species [71]. Thus, probing surface acidity with reducing probe molecules will alter the surface Brønsted acidity properties of the supported vanadia catalysts [23]. In contrast to the above supported vanadia catalysts, neither surface Brønsted nor Lewis acid sites are detected for surface vanadia on

SiO_2 [72]. The absence of surface Brønsted acid sites for surface vanadia species on silica is in agreement with the acidic properties of other well-dispersed oxides on silica [66], and suggests that the presence of surface Brønsted acid sites occasionally reported for silica-supported vanadia catalysts must be attributed to the presence of microcrystalline V_2O_5 or surface impurities. In summary, both the surface vanadia species and the microcrystalline V_2O_5 possess surface Brønsted acid sites, but surface vanadia species on SiO_2 do not possess surface Brønsted acid sites. High activity and low selectivity of supported vanadia catalysts in *n*-butane ODH to C_4-olefins at low surface coverages is explained by the high Brønsted acid character of octahedral V(V) species [19].

Supported VPO catalysts typically exhibit surface enrichment in phosphate similar to the conventional unsupported or bulk VPO catalysts [1–16]. In these catalysts the concentration of the surface Brønsted acid sites increases with the surface P/V ratio. The surface enrichment in phosphorus stabilizes the V(IV) oxidation state, which results in decreased activity in *n*-butane oxidation. On the other hand, the increased surface Brønsted acidity facilitates desorption of partially oxidized products with acidic properties, such as maleic anhydride, leading to significant improvement in maleic anhydride selectivity [2,11,14,16]. According to Grasselli et al. [73], slight excess phosphate (P/V=1.1–1.2) forms a protective pyrophosphate "fence" around active surface sites at the surface preventing overoxidation of the reactive intermediates by the active oxygen diffusing fast at the surface. However, the changes in the activity and selectivity of the VPO catalysts at much higher phosphorus enrichment (P/V ratio near 2.0) were associated with formation of microcrystalline $VO(PO_3)_2$ [57]. Reports in the literature have demonstrated that the $VO(PO_3)_2$ phase is inactive in *n*-butane oxidation [15,57]. Therefore, the catalytic behavior of the $VO(PO_3)_2$ system is explained by the presence of other VPO impurity phases, such as $(VO)_2P_2O_7$ and various $VOPO_4$ phases [15,57]. The oxidation of *n*-butane on well-defined supported vanadia catalysts [11] demonstrated that the substitution of V–O–Ti for less reducible and more acidic V–O–P bonds has a positive effect on the *n*-butane oxidation TOF and maleic anhydride selectivity. This observation indicates that the oxidation of *n*-butane to maleic anhydride requires both a redox site and some acidic functionality.

8. Lessons for unsupported VPO system

Oxidation of *n*-butane on the unsupported or bulk VPO catalysts is the only known commercial process for an alkane oxidation. A number of V(IV) and V(V) phosphates exist in the VPO system and the correlation of catalytic performance with crystalline structure has been reviewed [74–78]. Vanadyl(IV) pyrophosphate, $(VO)_2P_2O_7$, has been identified as critical for active and selective industrial catalysts [77]. Some argue that the V(V)/V(IV) dimeric species in the topmost oxidized layer of $(VO)_2P_2O_7$ are the active sites [73,79–81], while others believe that the active sites lie within the microdomains of crystalline vanadyl(V) orthophosphates, β-, α_{II}-, γ-, and δ-$VOPO_4$, or vanadyl(IV) metaphosphate, $VO(PO_3)_2$, formed on the (1 0 0) faces of vanadyl pyrophosphate under the catalytic reaction conditions [1,82–86]. A recent kinetic study demonstrated that the best bulk VPO catalysts contained only crystalline vanadyl(IV) pyrophosphate after reaching the steady state [57]. The vanadyl(IV) pyrophosphate phase displayed preferential exposure of the (1 0 0) planes which contain vanadyl dimers associated with active sites for *n*-butane oxidation [57]. A high-resolution electron microscopy study demonstrated that the surface (1 0 0) planes in the fresh catalysts are covered with ca. 1.5 nm amorphous layered which completely disappears within 23 days of *n*-butane oxidation [87]. The kinetic studies of the bulk VPO catalysts further demonstrated the similarity between the unsupported VPO catalysts and supported catalytic systems. The catalytic activity of the unsupported VPO catalysts was confined to a very thin surface region of the (1 0 0) crystalline planes of vanadyl(IV) pyrophosphate (1–2 atomic layers) [88].

These findings suggested that the crystalline vanadyl(IV) pyrophosphate phase in the bulk VPO catalysts functioned as a support for the active surface. Such $(VO)_2P_2O_7$ support stabilized some specific surface termination of the (1 0 0) planes with V^{4+}/V^{5+} species and phosphate groups without contributing its lattice oxygen to *n*-butane oxidation. Unfortunately, various spectroscopic techniques, such as Raman,

NMR, ESR, UV–Vis DRS, IR and EXAFS/XANES, are unable to provide information about the molecular structure of the surface present in the bulk VPO catalysts because of the much stronger signals from the catalyst bulk than the catalyst surface [53]. Limitations of both the bulk and surface characterization techniques currently available, coupled with the complex solid-state chemistry of vanadium phosphates, have led to considerable confusion and contradictions in the literature concerning the identity of the active sites involved in different steps of *n*-butane oxidation to maleic anhydride over the unsupported VPO catalysts [53].

Unlike bulk VPO catalysts, detailed surface structural information on a molecular level can be obtained from model supported vanadia catalysts containing two-dimensional overlayers of surface vanadia species [21,89–92]. Raman spectroscopy provides direct fundamental surface information about

1. the ratio of isolated and polymerized surface vanadia species (Fig. 1),
2. terminal V=O and bridging V–O–V bonds,
3. extent of reduction of the surface vanadia species during catalysis,
4. influence of the oxide support ligands, and
5. influence of acidic/basic metal oxide additives (promoters/poisons) and participation of specific V–O bonds in catalysis (with the aid of oxygen-18 labeled isotope experiments).

Thus, the in situ Raman studies during oxidation of reactions over model supported vanadia catalysts can provide new insights into the surface properties of oxide catalysts which are not attainable with bulk metal oxide catalysts.

The studies of the model supported catalysts provided several important insights about the origins of the catalytic activity of the VPO system that were not possible with the bulk VPO catalysts [11,16]. Firstly, it was shown that the V=O oxygen was not involved in *n*-butane oxidation to maleic anhydride and that the V–O-support bonds contained active oxygen for *n*-butane oxidation. The V–O–P bonds were particularly beneficial for both the activity and selectivity of the supported vanadia catalysts (Table 3 [16]), suggesting that this oxygen species may be responsible for selective oxidation of *n*-butane. Secondly, it was demonstrated that the oxidation of *n*-butane to maleic anhydride could occur at a single vanadia site, although adjacent sites were more efficient (Fig. 11 [16]). In the case of the bulk VPO system, the vanadyl(IV) dimers present in the crystalline (1 0 0) planes of $(VO)_2P_2O_7$ were associated with the active sites for selective oxidation of *n*-butane in several hypothetical models [78]. The kinetic studies of the supported vanadia system [11,16] provided a more direct evidence that the multiple vanadia sites were better at oxidizing *n*-butane to maleic anhydride.

Lastly, the use of acidic additives with supported VPO catalysts further demonstrated their similarity to the bulk VPO system. Moreover, it shed some light on the possible role of promoters that improve the performance of the bulk VPO catalysts [16,93]. The acidic additives used in the supported vanadia catalysts enhance those catalytic oxidations which require a combination of a redox and acidic site for selective catalysis. The acidic additives promoted both the rate of *n*-butane oxidation and the maleic anhydride formation on supported vanadia catalysts (Table 3 [16]). In the case of the unsupported VPO catalysts, the role of alkali and alkaline earth metal ion promoters (Li, Na, K, Cs, Be, Mg, Ca, and Ba) in the oxidation of *n*-butane to maleic anhydride has been recently studied by Haber et al. [93]. In this study, the selectivity to maleic anhydride also correlated with the concentration of the acidic sites on the surface, passing through a maximum as the concentration of acid sites increased (Fig. 6 [93]). Surface acidity expressed in the amount of adsorbed ammonia correlated best with the surface [O/(V+P+Me)] ratio (Fig. 3 [93]), implying that besides the P–OH groups, the surface contained different acidic OH groups capable of adsorbing ammonia. Haber et al. [93] believed that the surface acidic sites affect selectivity by controlling adsorption of the reaction intermediates and maleic anhydride which possess acidic properties. At low surface acidity, the desorption of the adsorbed acid-like products is hindered, and they are overoxidized to CO_x. At high surface acidity, the acidic reaction intermediates are desorbed from the surface before they are oxidized further into maleic anhydride.

The supported V(PO) system proved to be a good model for the bulk, i.e. unsupported, VPO system. The in situ Raman studies of the supported vanadia catalysts [11,14–17,58] provided several important insights into the nature of the selective *n*-butane

oxidation that were not possible with unsupported VPO catalysts due to the experimental limitations [53]. The many discovered similarities between the bulk and supported VPO systems have important implications for the design of new selective V(PO) catalysts [11,16,59]. The nature of the oxide support, the surface coverage of the active vanadia species and the acidity of metal oxide additive are the most important determinants of the catalytic activity and selectivity in *n*-butane oxidation. These structure–reactivity relationships pave the way for molecular engineering of selective active sites for hydrocarbon oxidation in supported V(PO) catalysts.

9. Conclusions

Significant progress has been achieved in recent years in studying molecular structures of the surface vanadia species present in supported metal oxide catalysts. The detailed structural information on well-defined systems provided a foundation for developing structure–reactivity relationships required to molecularly engineer supported vanadia catalysts for oxidation reactions. The nature of the metal oxide support is found to play a crucial role in defining catalytic properties of vanadia monolayers in *n*-butane oxidation to maleic anhydride. The terminal vanadyl oxygen does not appear to critically influence the reactivity properties of the surface vanadia species during hydrocarbon oxidation reactions. The bridging V–O–V oxygen plays only a minor role in enhancing the *n*-butane oxidation TOF, primarily due to the preference of multiple active sites in this oxidation reaction. The bridging V–O-support oxygen, however, appears to be the most critical oxygen since its properties can change the TOF for hydrocarbon oxidation reactions by as much as four orders of magnitude. The specific phase of the oxide support as well as the specific preparation method do not appear to influence the molecular structure or reactivity of the surface vanadia species. The number of surface vanadia sites required for a hydrocarbon oxidation reaction is dependent on the specific reactant molecule. Oxidation reactions requiring only one surface vanadia site are generally not sensitive to the surface vanadia coverage and the presence of noninteracting metal oxides. Oxidation reactions requiring multiple surface vanadia sites are very sensitive to surface vanadia coverage and the presence of noninteracting metal oxides. However, interacting metal oxides influence all hydrocarbon oxidation reactions since they modify the surface vanadia sites. Acidic and basic metal oxides also influence the selectivity of hydrocarbon oxidation reactions, but the effect appears to be reaction-specific.

The results of *n*-butane oxidation on titania-supported vanadia catalysts suggested that isolated surface vanadia species are capable of *n*-butane oxidation to maleic anhydride, although multiple vanadia sites are more efficient in this oxidation. Microcrystalline vanadia was found to be detrimental for the process of maleic anhydride formation.

The selectivity of the supported catalysts to maleic anhydride correlated with the Lewis acid strength of the metal oxide promoters. Especially high selectivity to maleic anhydride was found when the V–O–P bonds formed after addition of phosphorus oxide in accordance with previous observations in supported and unsupported bulk VPO catalysts. These findings indicate that the supported vanadia catalysts represent a suitable model system capable of providing insights into the mechanism of *n*-butane oxidation on bulk VPO catalysts.

The new fundamental insights into the structure and reactivity of surface vanadia species on oxide supports provide a foundation for the molecular engineering of supported catalysts for selective hydrocarbon oxidation. Furthermore, these insights are also assisting the development of a sound theoretical foundation in the area of C_4 hydrocarbon oxidation.

References

[1] M. Nakamura, K. Kawai, Y. Fujiwara, J. Catal. 34 (1974) 345.
[2] V.A. Zazhigalov, Y.P. Zaitsev, V.M. Belousov, B. Parlitz, W. Hanke, G. Öhlman, React. Kinet. Catal. Lett. 32 (1989) 209.
[3] A. Ramstetter, M. Baerns, J. Catal. 109 (1988) 303.
[4] R.L. Varma, D.N. Saraf, Ind. Chem. Eng. 20 (1978) 42.
[5] P.S. Kuo, B.L. Yang, J. Catal. 117 (1989) 301.
[6] M. Martinez-Lara, L. Moreno-Real, R. Pozas-Tormo, A. Jimenez-Lopez, S. Bruque, P. Ruiz, G. Poncelet, Can. J. Chem. 70 (1992) 5.
[7] M. Derewinski, J. Haber, R. Kozlowski, W.A. Zazhigalov, J.P. Zajtsev, I.W. Bacherikowa, W.M. Belousov, Bull. Polish Acad. Sci. Chem. 39 (1991) 403.

[8] M. Ruitenbeek, R.A. Overbeek, A.J. van Dillen, D.C. Koningsberger, J.W. Geus, Recl. Trav. Chim. Pays-Bas 115 (1996) 519.
[9] R.A. Overbeek, P.A. Warringa, M.J.D. Crombag, L.M. Visser, A.J. van Dillen, J.W. Geus, Appl. Catal. A 135 (1996) 209.
[10] R.A. Overbeek, A.R.C.J. Pekelharing, A.J. van Dillen, J.W. Geus, Appl. Catal. A 135 (1996) 231.
[11] I.E. Wachs, J.-M. Jehng, G. Deo, B.M. Weckhuysen, V.V. Guliants, J.B. Benziger, Catal. Today 32 (1996) 47.
[12] M. Ruitenbeek, R.A. Overbeek, D.C. Koningsberger, J.W. Geus, in: E.G. Derouane et al. (Eds.), Catalytic Activation and Functionalization of Light Alkanes, Kluwer Academic Publishers, Dordrecht, 1998.
[13] W.D. Harding, K.E. Birkeland, H.H. Kung, Catal. Lett. 28 (1994) 1.
[14] K.E. Birkeland, S.M. Babitz, G.K. Bethke, H.H. Kung, G.W. Coulston, S.R. Bare, J. Phys. Chem. B 101 (1997) 6895.
[15] G.K. Bethke, D. Wang, J.M.C. Bueno, M.C. Kung, H.H. Kung, The Third World Congress on Oxidation Catalysis, Elsevier, Amsterdam, 1997, p. 453.
[16] I.E. Wachs, J.-M. Jehng, G. Deo, B.M. Weckhuysen, V.V. Guliants, J.B. Benziger, S. Sundaresan, J. Catal. 170 (1997) 75.
[17] L. Owens, H.H. Kung, J. Catal. 144 (1993) 202.
[18] E.A. Mamedov, V.C. Corberan, Appl. Catal. A 127 (1995) 1.
[19] T. Blasco, A. Galli, J.M.L. Nieto, F. Trifiró, J. Catal. 169 (1997) 203.
[20] G. Deo, I.E. Wachs, J. Haber, Critical Rev. Surf. Chem. 4 (1994) 141.
[21] I.E. Wachs, Catal. Today 27 (1996) 437.
[22] G.C. Bond, Appl. Catal. 71 (1991) 1.
[23] G.C. Bond, J.C. Vedrine, Catal. Today (special issue) (1994) 20.
[24] G. Deo, I.E. Wachs, J. Catal. 146 (1994) 323.
[25] J.M.L. Nieto, G. Kremenic, J.L.G. Fierro, Appl. Catal. 61 (1990) 235.
[26] G. Deo, I.E. Wachs, J. Catal. 146 (1994) 335.
[27] I.E. Wachs, R.Y. Saleh, S.S. Chan, C.C. Chersich, Appl. Catal. 15 (1985) 339.
[28] M.M. Koranne, J.G. Goodwin Jr., G. Marcelin, J. Catal. 148 (1994) 369.
[29] G.C. Bond, K. Bruckman, Faraday Disc. Chem. Soc. 72 (1981) 235.
[30] J. Haber, T. Machej, E.M. Serwicka, I.E. Wachs, Catal. Lett. 32 (1995) 101.
[31] N. Das, H. Eckert, H. Hu, I.E. Wachs, J.F. Walzer, F.J. Feher, J. Phys. Chem. 97 (1993) 8240.
[32] H. Eckert, I.E. Wachs, J. Phys. Chem. 93 (1989) 6796.
[33] G. Busca, E. Giamello, Mater. Chem. Phys. 25 (1990) 475.
[34] B.M. Weckhuysen, I.P. Vannijvel, R.A. Schoonheydt, Zeolites 15 (1995) 482.
[35] R.A. Overbeek, E.J. Bosma, D.W.H. de Blauw, A.J. van Dillen, H.G. Bruil, J.W. Geus, Appl. Catal. A 163 (1997) 129.
[36] M. De Boer, R.G. Leliveld, A.J. van Dillen, J.W. Geus, H.G. Bruil, Appl. Catal. A 102 (1993) 35.
[37] T. Machej, J. Haber, A.M. Turek, I.E. Wachs, Appl. Catal. 70 (1991) 115.
[38] G. Busca, Mater. Chem. Phys. 19 (1988) 157.
[39] A.A. Davydov, Kinet. Katal. 34 (1993) 951.
[40] G.T. Went, S.T. Oyama, J. Phys. Chem. 94 (1990) 4240.
[41] S.C. Su, A.T. Bell, J. Phys. Chem. B 102 (1998) 7000.
[42] J. Hanuza, B. Jezowska-Trzebiatowska, W. Oganowski, J. Mol. Catal. 29 (1985) 109.
[43] R. Kozlowski, R.F. Pettifer, J.M. Thomas, J. Phys. Chem. 87 (1983) 5176.
[44] K. Inumaru, M. Misono, T. Okuhara, Appl. Catal. A 149 (1997) 133.
[45] I.E. Wachs, G. Deo, A. Andreini, M.A. Vuurman, M. de Boer, M. Amiridis, J. Catal. 161 (1996) 211.
[46] G. Ramis, C. Cristiani, P. Forzatti, G. Busca, J. Catal. 116 (1990) 574.
[47] S. Takenaka, T. Tanaka, T. Yamazaki, T. Funabiki, S. Yoshida, J. Phys. Chem. B 101 (1997) 9035.
[48] Q. Sun, H. Hu, R.G. Herman, I.E. Wachs, K. Klier, J. Catal. 165 (1997) 91.
[49] J.-M. Jehng, H. Hu, X. Gao, I.E. Wachs, Catal. Today 28 (1996) 335.
[50] I.E. Wachs, B.M. Weckhuysen, Appl. Catal. A 157 (1997) 67.
[51] M.A. Eberhardt, A. Proctor, M. Houalla, D.M. Hercules, J. Catal. 160 (1996) 27.
[52] M.C. Paganini, L. Dall'Acqua, E. Giamello, L. Lietti, P. Forzatti, G. Busca, J. Catal. 166 (1997) 195.
[53] G. Centi (Ed.), Proceedings, Vanadyl Pyrophosphate Catalysts, Catalysis Today, Elsevier, Amsterdam, vol. 16, 1993, pp. 1–154.
[54] K. Mori, A. Miyamoto, Y. Murakami, J. Phys. Chem. 89 (1985) 4265.
[55] G. Busca, G. Centi, F. Trifirói, Appl. Catal. 25 (1986) 265.
[56] Z. Tvaruzkova, G. Centi, P. Jiru, F. Trifiró, Appl. Catal. 19 (1985) 307.
[57] V.V. Guliants, J.B. Benziger, S. Sundaresan, I.E. Wachs, J.-M. Jehng, Catal. Today 28 (1996) 275.
[58] J.M.C. Bueno, G.K. Bethke, M.C. Kung, H.H. Kung, Catal. Today 43 (1998) 101.
[59] I.E. Wachs, Catalysis 2 (1997) 37.
[60] R.T. Sanderson, Polar Covalence, Academic Press, New York, 1983.
[61] P.L. Gai, K. Kourtakis, Science 267 (1995) 661.
[62] M.A. Vuurman, I.E. Wachs, J. Mol. Catal. 77 (1992) 29.
[63] G. Ramis, G. Busca, F. Bregani, Catal. Lett. 18 (1993) 299.
[64] B. Grzybowska, P. Mekss, R. Grabowski, K. Wcislo, Y. Barbaux, L. Gengembre, Stud. Surf. Sci. Catal. 82 (1994) 151.
[65] G. Busca, G. Ramis, V. Lorenzelli, J. Mol. Catal. 50 (1989) 231.
[66] J. Datka, A.M. Turek, J.-M. Jehng, I.E. Wachs, J. Catal. 135 (1992) 186.
[67] H. Miyata, K. Fuji, T. Ono, J. Chem. Soc., Faraday Trans. 84 (1988) 3121.
[68] V.M. Mastikhin, A.V. Nosov, V.V. Terskikh, K.I. Zamaraev, I.E. Wachs, J. Phys. Chem. 98 (1994) 13621.
[69] G. Busca, L. Marchetti, G. Centi, F. Trifiró, J. Chem. Soc., Faraday Trans. 81 (1985) 1003.

[70] N.-Y. Topsoe, H. Topsoe, J.A. Dumesic, J. Catal. 151 (1995) 226.
[71] K. Segawa, W.K. Hall, J. Catal. 76 (1982) 133.
[72] I.E. Wachs, G. Deo, A. Andreini, M.A. Vuurman, M. de Boer, M. Amiridis, J. Catal. 161 (1996) 211.
[73] P.A. Agaskar, L. DeCaul, R.K. Grasselli, Catal. Lett. 23 (1994) 339.
[74] E. Bordes, Catal. Today 1 (1987) 499.
[75] P. Amorós, R. Ibánez, E. Martínez-Tamayo, A. Beltrán-Porter, D. Beltrán-Porter, G. Villeneuve, Mater. Res. Bull. 24 (1989) 1347.
[76] G. Centi, F. Trifirò, J.R. Ebner, V.M. Franchetti, Chem. Rev. 88 (1988) 55.
[77] G. Centi, Catal. Today 16 (1993) 5.
[78] F. Cavani, F. Trifirò, CHEMTECH 24 (1994) 18.
[79] B.K. Hodnett, Catal. Rev., Sci. Eng. 27 (1985) 373.
[80] G. Centi, F. Trifirò, Chim. Ind. (Milan) 68 (1986) 74.
[81] B.K. Hodnett, Catal. Today 1 (1987) 477.
[82] N. Harrouch Batis, H. Batis, A. Ghorbel, J.C. Vedrine, J.C. Volta, J. Catal. 128 (1991) 248.
[83] M. Guilhoume, M. Roullet, G. Pajonk, J.C. Volta, in: P. Ruiz, B. Delmon (Eds.), New Developments in Selective Oxidation by Heterogeneous Catalysts, Elsevier, Amsterdam, vol. 255, 1992.
[84] J.C. Vedrine, J.M.M. Millet, J.C. Volta, Faraday Discuss. Chem. Soc. 87 (1989) 207.
[85] H. Morishige, J. Tamaki, N. Miura, N. Yamazoe, Chem. Lett. (1990) 1513.
[86] N. Yamazoe, H. Morishige, J. Tamaki, N. Miura, New Frontiers in Catalysis, L. Guczi (Ed.), Elsevier, Amsterdam, 1993, 1979.
[87] V.V. Guliants, J.B. Benziger, S. Sundaresan, N. Yao, I.E. Wachs, Catal. Lett. 32 (1995) 379.
[88] M.A. Pepera, J.L. Callahan, M.J. Desmond, E.C. Milberger, P.R. Blum, N.J. Bremer, J. Am. Chem. Soc. 107 (1985) 4883.
[89] J.M. Stencel, Raman Spectroscopy for Catalysis, van Nostrand Reihold, New York, 1990.
[90] J.G. Grasselli, B.J. Bulkin (Eds.), Analytical Raman Spectroscopy, Wiley, New York, 1991.
[91] I.E. Wachs, F.D. Hardcastle, Catalysis, Royal Society of Chemistry, Cambridge, UK, vol. 10, 1993, p. 102.
[92] I.E. Wachs, K. Segawa, in: I.E. Wachs (Ed.), Characterization of Catalytic Materials, Butterworths, Stoneham, MA, 1992, p. 69.
[93] V.A. Zazhigalov, J. Haber, J. Stoch, I.V. Bacherikova, G.A. Komashko, A.I. Pyatnitskaya, Appl. Catal. A 134 (1996) 225.